Kinetic Effects on Resistive Wall Mode Stability

T C Hender[a], I T Chapman[a], M S Chu[b] and Y-Q Liu[a]

[a]*EURATOM/UKAEA Fusion Association, Culham Science Centre, Abingdon, Oxon OX14 3DB, UK*
[b]*General Atomics, P.O. Box 85608, San Diego, California 92186-5608, USA*

Abstract. Two approaches for studying the damping of resistive wall modes due to wave particle resonant interactions are discussed. One approach uses the eigenfunction from an ideal MHD code combined with the resonant particle damping calculated from a drift-kinetic δf - method formulation. This perturbative approach treats the wave-particle interaction precisely, but does not include the back-effect of the kinetic terms on the eigenfunction structure. In the alternate non-perturbative approach the kinetic terms are included in an MHD description via the pressure tensor. This non-perturbative approach includes the resonances due to the bounce and precessional drifts subject to certain approximations. Comparisons between the two approaches and conclusions on the dominant stabilizing mechanisms are presented.

Keywords: Tokamak, Resistive Wall Mode
PACS: 52.25.Dg, 52.55.Fa, 52.65.Kj, 52.35.Bj

INTRODUCTION

The ultimate performance limit is set by Resistive Wall Modes (RWMs) [1] in advanced tokamak operating scenarios, such as those foreseen for ITER and compatible with the steady-state operation of a power plant. The RWM is a kink mode whose stability is related to damping arising from relative rotation between the (possibly) fast rotating plasma and the slowly rotating wall mode. Plasma rotation, and the ensuing RWM damping, is a passive stabilising mechanism making it an attractive route for RWM control. It is thus important to understand how plasma rotational stabilisation of the RWM will scale to future devices. The nature of this stabilisation is still under study and several models have been proposed, e.g. an empirical sound wave damping model [1] and a 'semi-kinetic' model [2] which has no free fitting parameters. A range of other damping models and mechanisms have also been proposed, e.g. [3-8]. The theory development is being driven by experimental observations of RWM stability at very low rotation in balanced neutral beam injection (NBI) experiments in the DIII-D [9] and JT-60U [10] tokamaks.

This paper discusses some areas of recent progress in developing new models for RWM damping. The drift-orbit particle-following HAGIS code [11] is being used in a perturbative manner to study kinetic resonance damping effects based on single fluid external kink eigenfunctions. This gives an exact treatment of the kinetic damping terms, but does not self consistently include the effect of the kinetic terms on the

CP1069, *Theory of Fusion Plasmas, Joint Varenna-Lausanne International Workshop*
edited by X. Garbet, O. Sauter, and E. Sindoni

eigenmode structure. To attain a more self-consistent formulation the MARS linear MHD stability code [12] has been extended to include the kinetic damping terms in a non-perturbative manner. The drift kinetic equation for the perturbed distribution function is solved analytically to give the perturbed kinetic pressures, for inclusion in the MHD equations. The effects of the particle bounce resonance and precession drift resonance, for both passing and trapped particles, and ions and electrons (where appropriate), are included. The drift orbit formulation using the HAGIS code is described in the next section, and then in the following section the formulation and results with the non-perturbative hybrid kinetic-MHD code, MARS-K are discussed.

PERTURBATIVE APPROACH

In the perturbative approach the external kink eigenfunction is taken from the ideal MHD code MISHKA [13] and this is used to calculate the change to the perturbed potential energy from the kinetic terms (δW_k) using the HAGIS code [11] for a prescribed ion (and possibly electron) distribution function. If δW_f is the MHD potential energy (here computed with the MISHKA code) then the growth rate (γ) of the RWM is given by [4,14]:-

$$\gamma\tau_W = -\frac{\delta W_f^{\infty} + \delta W_k}{\delta W_f^{b} + \delta W_k} \tag{1}$$

where τ_W is the resistive wall time of a wall at $r=b$ (see [14] for a full definition) and the superscript ∞ denotes no-wall (i.e. wall at $r=\infty$). For an RWM by assumption $\delta W_f^{\infty} < 0$ and $\delta W_f^{b} > 0$. The perturbed kinetic energy is defined in terms of the perturbed anisotropic pressure as

$$\delta W_k = \frac{1}{2}\int \nabla\cdot\left(\delta P_{\perp}\underline{\underline{I}} + \left[\delta P_{\parallel} - \delta P_{\perp}\right]\underline{bb}\right)\cdot\xi^* d^3x \tag{2}$$

which can be expressed in terms of the perturbed distribution function (δf) [15,16]

$$\delta W_k = \frac{1}{2}\int \left(mv_{\parallel}^2 + \mu B\right)\,\delta f\;\kappa\cdot\xi^* d^3x\, d^3v \tag{3}$$

where $\boldsymbol{\kappa}=\boldsymbol{b}.\nabla\boldsymbol{b}$ is the magnetic curvature. The perturbed distribution function is computed from the Vlasov equation using the δf-method [17] in the HAGIS code. In this method the total distribution function is split into a static and time varying part

$$f = f_0(P_{\xi}, \varepsilon, \mu) + \delta f(\Gamma, t) \tag{4}$$

where Γ represents six-dimensional phase space, P_{ξ} is the canonical angular momentum, ε is the energy, μ is the magnetic moment, f_0 is prescribed analytically and δf is represented by a large number of marker particles. In a collisionless formulation $df/dt=0$ and so

$$\frac{d\delta f}{dt} = -\frac{dP_{\xi}}{dt}\frac{\partial f_0}{\partial P_{\xi}} - \frac{d\varepsilon}{dt}\frac{\partial f_0}{\partial \varepsilon} \tag{5}$$

The marker particles in HAGIS are advanced using the guiding centre equations of motion and their weighting is determined according to Eq. (5).

The particle-mode resonances giving rise to the kinetic damping (or drive) on the RWM are given by [18]

$$\omega - \Omega - n\left\langle \dot{\phi} \right\rangle - l\left\langle \dot{\theta} \right\rangle = 0 \tag{6}$$

where $\left\langle \dot{\phi} \right\rangle$ is the orbit averaged toroidal motion of the particle, $\left\langle \dot{\theta} \right\rangle$ is the poloidal motion, n is the toroidal mode number, ω is the mode frequency, Ω is the plasma rotation frequency and l is an integer; for the RWM $\omega \tau_{W} \lesssim 1$, so that in general $\omega << \Omega$. As an example we show these resonances (Eq. 6) for a JET equilibrium (pulse 68875 at t=5s); this pulse does not have an RWM but resonant field amplification measurements [19] do suggest it exceeds the no-wall limit. The resonances for pulse 68875 are shown in Fig. 1.

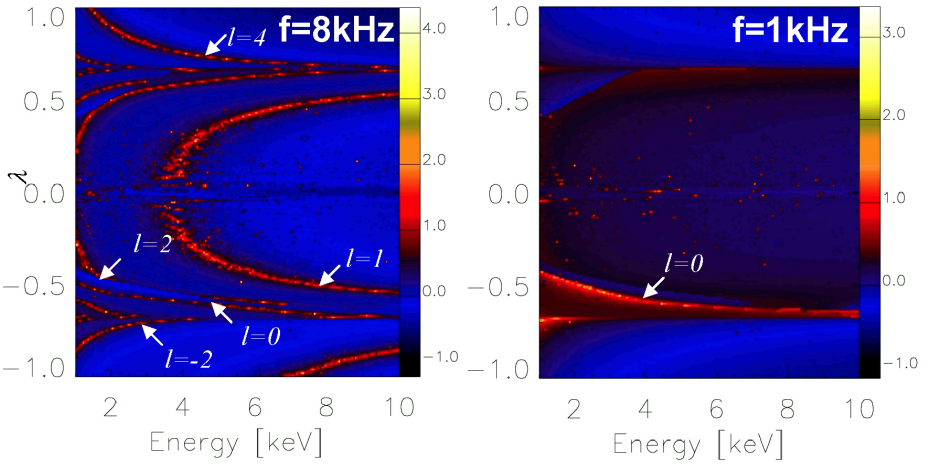

FIGURE 1. Mode-particle resonances, shown as contour of $1./\log\left(\omega - \Omega - n\left\langle \dot{\phi} \right\rangle - l\left\langle \dot{\theta} \right\rangle\right)$, in terms of pitch angle ($\lambda = v_{||}/v$) versus energy space. Here results are shown for $f=(\omega-\Omega)/2\pi$=8kHz and 1kHz.

In Fig.1 some of the resonances are identified. At low frequency (1kHz) the only significant resonance is the $l = 0$ precessional drift resonance, whereas at higher frequency (8kHz) bounce and passing particle resonances come into play. The damping from δW_k thus shows 2 peaks in the experimental range of plasma toroidal frequencies (<50krads^{-1} from the edge to mid-radius) associated with the precessional (ω_d) and bounce frequencies (ω_b) (Fig. 2) – the passing particle transit frequency is much higher. The effect of this resonant damping on mode stability is shown in Fig. 3; it can be seen that the kinetic damping raises the with-wall β-limit by about 35% (in C_β) and substantially lowers the growth rate. This calculation includes the thermal ion and electron distributions and the energetic ion distribution from neutral beam injection, calculated by the TRANSP code [20]. The rotation profile is taken from experimental charge exchange measurements.

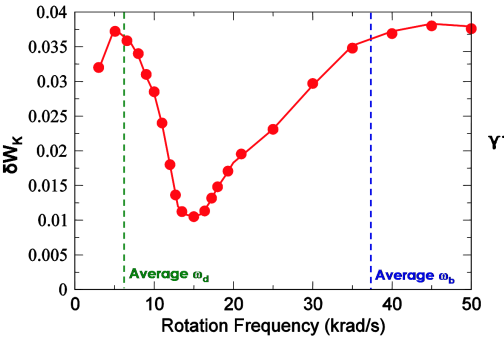

FIGURE 2. Change in kinetic potential energy versus plasma rotation frequency for the JET case, pulse 68875 at t=5s. The precessional drift (ω_d) and the particle bounce frequency (ω_b), averaged over the distribution, are marked.

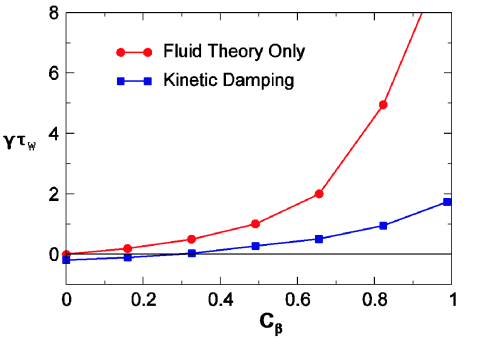

FIGURE 3. Growth rate (normalised by wall time) for the fluid only theory (wall at the JET vacuum vessel) and including the kinetic damping terms for the JET case, pulse 68875 at t=5s. Here C_β= (β_N-β_N(no-wall))/ (β_N(with-wall)-β_N(no-wall)).

NON-PERTURBATIVE APPROACH

In this approach the MARS linear MHD code [12] has been modified to include the kinetic terms, allowing a non-perturbative solution [21] (but with less generality over the kinetic terms than the approach discussed above). The key ingredient is to include the anistropic perturbed pressure into the linearised equation of motion:-

$$\rho(\gamma + in\Omega)\mathbf{v} = -\nabla\cdot\mathbf{P} + j\times B + J\times Q - \rho\left[2\Omega\hat{z}\times\mathbf{v} + (\mathbf{v}\cdot\nabla\Omega)R^2\nabla\phi\right] \tag{7}$$

where the pressure tensor is written as

$$\mathbf{P} = \left[p + \mathbf{P}_\perp\right]\underline{\underline{I}} + \left[\mathbf{P}_\parallel - \mathbf{P}_\perp\right]\underline{b}\underline{b} \tag{8}$$

j and J are the perturbed and equilibrium current density, Q and B are the perturbed and equilibrium magnetic field, $\underline{b}$ the unit vector in the B-direction and ρ the mass density. The perturbed pressures are given by integrals over the perturbed distribution function (f_1^L , termed δf in the previous section), e.g.

$$p_\parallel e^{-i\omega t + in\phi} = \sum_{e,i}\int d\Gamma M v_\parallel^2 f_1^L \tag{9}$$

where M is the particle mass. The relationship between the perturbed distribution function and the components of the perturbed displacement perpendicular to the equilibrium magnetic field and the parallel component of the perturbed magnetic field, represented by the vector **X,** is given by

$$f_L^1 = -f_\varepsilon^0 \varepsilon_k e^{-i\alpha t + in\phi} \sum_{m,l} \mathbf{X_m H_{m,l}} \lambda_{m,l} e^{-in\bar{\phi}(t) + im\langle\phi\rangle t + il\omega_b t} \tag{10}$$

where $\mathbf{H_{m,l}}$ is a geometric term and

$$\lambda_{m,l} = \frac{n\left[\omega_{*N} + (\hat{e}_k - 3/2)\omega_{*T} + \omega_E\right] - \omega}{n\omega_d + \left[\alpha(m+nq) + l\right]\omega_b - i\nu_{eff} - \omega} \tag{11}$$

with α=0 for trapped particles and α=1 for passing particles. Here ω_d is the precessional drift frequency, ω_b the bounce frequency, ω_{*N} and ω_{*T} are the diamagnetic drift frequencies due to the density and temperature gradients and ω_E is the $E\times B$ drift frequency; full details of the derivation and notation are given in [22]. As is evident from Eq. (11) this formulation includes in a non-perturbative manner the Landau-type damping arising from the precessional and trapped bounce frequency resonances, as well including the effects of diamagnetic drifts and plasma flows on the resonances. Not included in the formulation are the anisotropy of equilibrium pressure, the perturbed electrostatic potential, the radial excursion of particle trajectory or FLR corrections to the particle orbit.

To test the new MARS-K code extensive benchmark tests have been made. For example, comparisons have been made with results from the perturbative approach (MISHKA+HAGIS) discussed in the previous section. For this comparison a circular boundary Soleviev equilibrium [23] with a/R = 0.2, κ = 1.0, q_0 = 1.2 is used; for n=1 this case has no rational surfaces inside the plasma (q_{edge} = 1.41). The normalised pressure is β_N = 3.13, which gives a marginal ideal wall position for the n = 1 ideal external kink stability of 1.27a. It should be noted that although the normalized pressure is high, this case with q_{edge}<2, remains a current driven instability. There is very good agreement between the fluid potential energy computed by MARS-K and MISHKA (Fig. 4). Only the unstable modes (δW_b < 0) are computed by both codes and so the potential energy is extrapolated from the unstable modes using an analytic fit.

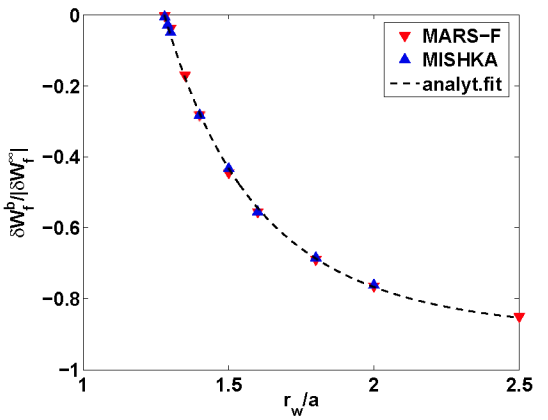

FIGURE 4. Comparison of the fluid potential energy with a wall δW_f^b, of the ideal kink mode computed by the MARS-K and MISHKA codes (normalized by the no-wall kink energy δW_f^∞) versus the radial position of an ideal wall.

Figures 5(a-b) compare the computed δW_k by MARS-K and by MISHKA+HAGIS, for the circular boundary Soloviev equilibrium; note for this benchmark comparison MARS-K is run in a perturbative manner so that the fluid eigenfunction is not modified by the kinetic terms. Also for this comparison just the ion energy is included in the stability calculation and the δW_k comes dominantly from the precession drift resonance with thermal trapped ions. The results in Fig. 5 show a scan in plasma rotation frequency with a uniform rotation profile. From Fig. 5 it can be seen that there is excellent agreement between the perturbative and non-perturbative approaches – indicating that the approximation made in the MARS-K formulation, that the banana width of trapped ions is neglected, is very satisfactory in this case. A comparison with the full precessional drift resonances, for both ion and electron, shows equally good agreement [22]. In Fig. 5 a broad range of frequencies is shown for benchmark purposes, beyond the likely physical range, including at very high frequency Alfvenic rotation where the Kruskal-Oberman terms dominate [24].

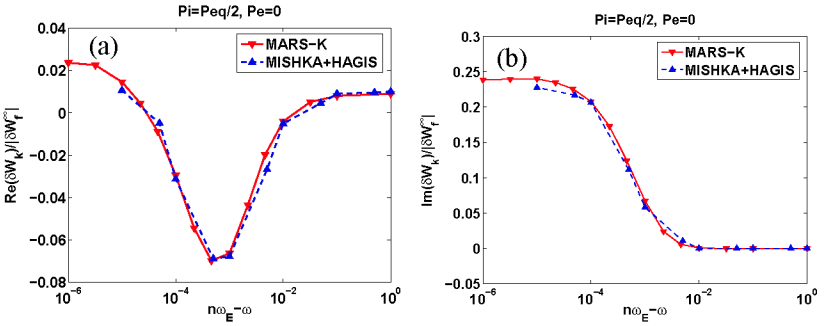

FIGURE 5. The (a) real, and (b) imaginary parts of the drift kinetic energy (normalized by fluid potential energy of the ideal kink mode with the wall at infinity), computed by the MARS-K and the HAGIS codes, respectively, versus the frequency of a uniform rotating plasma, for a circular boundary Soloviev equilibrium. For this comparison just the precessional drift resonances of the trapped thermal ions, are included. The ion gyro-frequency at the plasma centre is $\omega_{ci} = 121\omega_A$ (in these plots all frequencies are normalized to the Alfven time).

In Figs 6(a-b) the MISHKA+HAGIS and MARS-K results are compared in terms of the growth rate of the RWM versus the plasma rotation frequency. The growth rate is computed utilizing the RWM dispersion relation (Eq. 1) with a wall position of r_w = 1.15a. Comparing with the fluid growth rate (indicated by the solid line), only a slight variation of the RWM growth rate occurs due to the drift kinetic effects. In the comparison shown here only the ion precessional drift resonance is included; when the electron resonance is also included the comparison remains equally good, but a slight stabilization is realized for all mode frequencies [22].

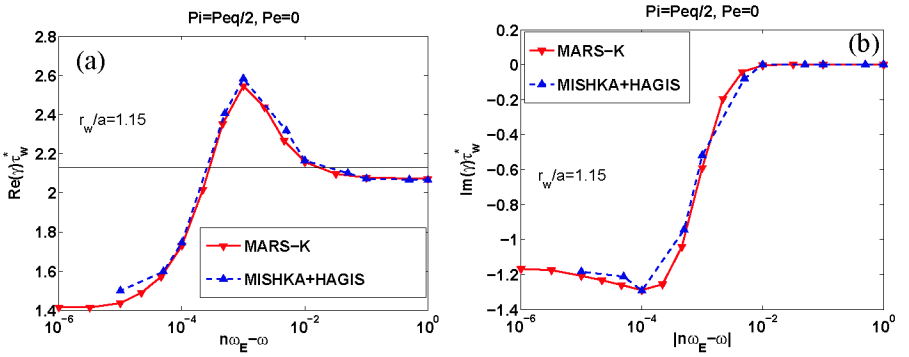

FIGURE 6. The (a) real, and (b) imaginary, parts of the kinetically modified RWM growth rate, computed by the MARS-K and the HAGIS codes, respectively, versus the frequency of a uniformly rotating plasma, for a circular-like Soloviev equilibrium. The precessional drift resonances from the trapped thermal ions are included. The wall position is at r_w = 1.15a. The ion gyro-frequency at the plasma centre is $\omega_{ci} = 121\omega_A$.

Having discussed some of the benchmark tests for MARS-K we now examine how the self-consistent non-perturbative eigenfunction structure affects the RWM results. As previously, a Soloviev equilibrium is used but now with an inverse aspect ratio a/R = 0.33, a plasma elongation of κ = 1.6, and a central q-value of 1.5 giving q_{edge} = 2.58. The instability is a mixture of a current and pressure-driven mode due to a fairly high β_N of 3.61. For the n=1 ideal kink the marginal ideal conformal wall radius is 1.21a. Figure 7 shows the growth rate versus wall position comparing the fluid growth rate, the non-perturbative self consistent (SC) solution and perturbative versions of the growth rate. For the perturbative solution the eigenfunction corresponding to the no-wall solution is employed and the mode growth rate from the fluid calculations is taken into account in the kinetic integrals. The non-perturbative approach shows a slight stabilisation of the mode close to the marginal wall position for the ideal kink, and a slight destabilisation at lower β_N. The results of self-consistent computations are quite different from the perturbative ones. We attribute this difference partly to the modification of the eigenmode structures in the self-consistent approach, as shown below. It should be noted that the effect of the kinetic corrections depends on the equilibrium and for realistic tokamak conditions we do find stabilisation of the RWM [25].

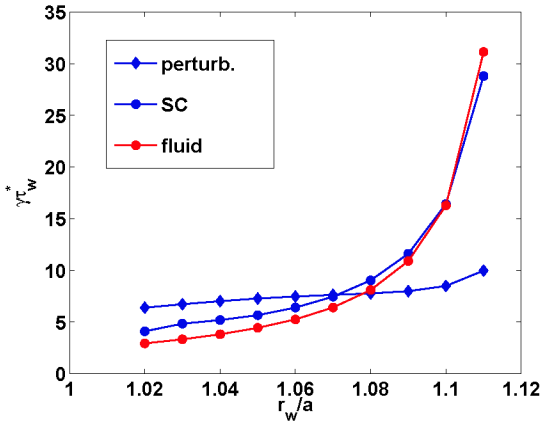

FIGURE 7. Comparison of the RWM growth rate versus the wall radius r_w under various assumptions. The eigenfunction of the ideal kink mode without wall is used in the perturbative approach and the plasma rotation is assumed to vanish. The ion gyro-frequency at the plasma centre $\omega_{ci} = 100\omega_A$ is assumed. Here 'SC' denotes the self-consistent solution.

The difference in the results between the perturbative and non-perturbative approaches is partly explained by the modification of the eigenmode structures due to the kinetic effects. Figures 8(a-c) display the parallel component of the perturbed kinetic pressure for a perturbative case with no rotation, a case including the fluid growth rate (as shown in Fig. 7) and from the non-perturbative self-consistent calculation also shown in Fig. 7. In the non-perturbative calculations, due to the kinetic modification of the mode eigenfunction, the perturbed kinetic pressure tends to be more localized at larger minor radius.

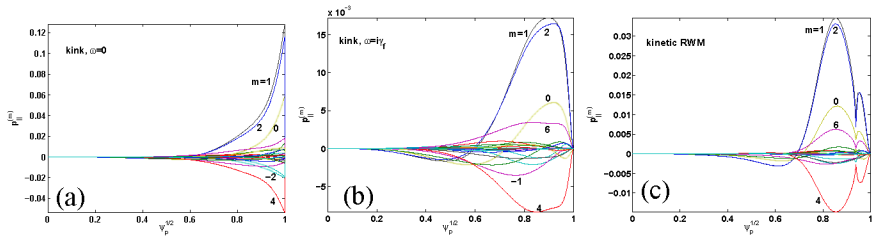

FIGURE 8. Poloidal Fourier harmonics of the perturbed parallel kinetic pressure, computed from (a) perturbative approach assuming vanishing mode frequency and growth rate in the kinetic integrals, (b) perturbative approach assuming vanishing mode frequency and fluid RWM growth rate, and (c) self-consistent approach. The wall minor radius is $r_w = 1.1a$. No plasma rotation is assumed. The edge zero values of the perturbed pressure in (b) and (c) are due to the vanishing edge equilibrium pressure – it should be noted that the plasma displacements remain finite at the edge in all cases.

SUMMARY

Resistive wall modes represent the ultimate performance limit in advanced tokamak scenarios. The stability of the resistive wall mode is thought to be determined by damping arising from plasma rotation relative to the slowly rotating RWM. A strong candidate for this rotational damping is due to wave-particle resonances. Two approaches to studying wave-particle damping of the RWM have been discussed. One approach uses the eigenfunction from the MISHKA ideal MHD code combined with the resonant particle damping calculated from the drift-kinetic δf-code, HAGIS. This perturbative approach treats the wave-particle interaction precisely but does not include the back-effect of the kinetic terms on the eigenfunction structure. In the alternate non-perturbative approach the kinetic terms are included in an MHD code description (MARS-K) via the pressure tensor. This non-perturbative approach includes the resonances due to the bounce and precessional drifts with some approximations but does resolve the effect of the kinetic damping terms on the eigenmode structure exactly. The perturbative approach shows for the JET example studied that the precessional drift and bounce resonances are dominant, and that these lead to a 15% increase in the β_N limit (above the no-wall limit). The non-perturbative approach has been benchmarked in appropriate limits by comparison with the perturbative HAGIS-MISHKA code formulation. It is found that the self consistent influence of kinetic terms on the eigenmodes is significant. In general in the cases examined so far, less kinetic stabilization is found in the self-consistent compared to the perturbative formulation. The methods discussed here are being applied to study RWM stability in DIII-D and JET, and will be used to predict RWM stability in ITER [25,26].

ACKNOWLEDGEMENTS

This work was funded by the United Kingdom Engineering and Physical Sciences Research Council, by the European Communities under the contract of Association between EURATOM and UKAEA, and by the US Department of Energy under contract DE-FG03-956ER54309. The views and opinions expressed herein do not necessarily reflect those of the European Commission. This work was conducted partly under the European Fusion Development Agreement. The authors thank the JET EFDA contributors for the JET data that is used.

REFERENCES

1. A. Bondeson and D. Ward, *Phys. Rev. Lett.* **72,** 2709 (1994)
2. A. Bondeson and M.S. Chu , *Phy.s of Plas.* **3,** 3013 (1996)
3. R. Fitzpatrick, Phys. of Plas. **9,** 3459 (2002)
4. Bo Hu and R. Betti, *Phys Rev Lett* **93**, 105002 (2004)
5. C.G. Gimblett, and R.J. Hastie, *Phys. of Plasmas* **7,** 258 (2000)
6. D. Gregoratto et al, Plasma Phys. *Contr. Fus.* **43,** 1425 (2001)
7. L.-J. Zheng, M. Kotschenreuther, and M.S. Chu, *Phys. Rev. Lett.* **95,** 255003 (2005)
8. Ph. Lauber and S. Günter, *Nucl. Fus.* **48** 084002 (2008)
9. H. Reimerdes et al, *Phys. Rev. Lett.* **98,** p.055001 (2007)

10. M. Takechi et al, *Phys. Rev. Lett.* **98,** p.055002 (2007)
11. S.D. Pinches et al, *Comput. Phys. Commun.* **111,** 133 (1998); HAGIS version 8.08 is used in this paper (from https://mastweb.fusion.org.uk/svnroot/hagis/releases/8.08/)
12. Y-Q. Liu et al., *Phys. Plasmas* **7,** 3681 (2000)
13. A.B. Mikhailovskii, G.T.A Huysmans, S.E. Sharapov and W.O. Kerner, *Plasma Phys. Rep.* **23,** 844 (1997)
14. S.W. Haney and J.P. Freidberg, *Phys. Fluids B* 1, 1637 (1989).
15. B.N. Breizman, J. Candy, F. Pocelli, and H. Berk, *Phys. Plasmas,* **5,** 2326 (1998)
16. F. Porcelli, R. Stankiewicz, W. Kerner, and H. L. Berk, *Phys. Plasmas,* **1,** 470 (1994)
17. S. E. Parker and W. W. Lee, *Phys. Fluids B* 5 77 (1993)
18. H.L. Berk, B.N. Breizman, and H. Ye, *Physics Letters A*, v.162 p.475 (1992)
19. M.P. Gryaznevich et al, 'Experimental Studies of Stability and Beta Limit in JET', submitted to *Plasma Phys. Contr. Fus.* 2008
20. R.J. Goldston et al, *J. Comp. Phys.* 43 61 (1981)
21. M.S. Chu and Y.Q. Liu, '*Modeling of Resistive Wall Mode with Full Kinetic Damping*' invited talk 2008 International Sherwood Theory Conference, Boulder, Colorado, USA, March 30-April 2, 2008
22. Y-Q Liu et al, 'Toroidal self-consistent modeling of drift kinetic effects on the resistive wall mode' submitted to *Phys. Plasmas*
23. L.S. Soloviev, '*Reviews of Plasma Phys.*', Vol 6, ed. M A Leontovich (Consultants Bureau, New York) pp. 257 (1975)
24. M.D. Kruskal and C.R. Oberman, Phys. Fluids **1** 275 (1958).
25. Y-Q. Liu et al, paper TH/P9-26, IAEA Fusion Energy Conf. 2008
26. I.T. Chapman et al, 'Kinetic Effects on the Resistive Wall Mode', to be submitted to *Plasma Phys. Contr. Fus.* (2008)